

Numerical Investigation of Aluminum Honey Comb Filled High Strength Steel Crash Box for the Effect of Honey Comb Physical Parameters on Crashworthiness Constant

ANNAMALAI, K and BALAJI, G.

¹ Professor, School of Mechanical and Building Sciences, VIT University, Chennai-600 127, Tamil Nadu, India

² Research Scholar, School of Mechanical and Building sciences, VIT University, Chennai-600 127, Tamil Nadu, India

balaji.g2014phd1139@vit.ac.in

Abstract

Fillers can be employed as reinforcement in the design of automobile crash boxes to improve its performance in terms of energy absorption, expected crushing fashion and initial peak force magnitude. The current research focuses on the investigation of crashworthiness of the high-strength steel (HSS) columns filled with reinforced aluminium honeycomb fillers. The crashworthiness of HSS steel crash boxes embedded with aluminium honeycomb of varying thickness and cell sizes are investigated. Five variants of honeycomb thickness, namely; Thickness-1, Thickness-2, Thickness-3, Thickness-4, Thickness-5 and six variants of honeycomb cell size, namely; CellSize-1, CellSize-2, CellSize-3, CellSize-4, CellSize-5 and CellSize-6 are considered for the crash box analysis. Numerical crash analysis is performed for the novel reinforced sandwich honeycomb separated by steel plates in HSS crash box. A further study is also performed by inducing V-Notch triggers in the honeycomb to evaluate the effect of crashworthiness parameters. A comparative numerical investigation is performed to realize the effect of geometric parameters on the crashworthiness variables of crash boxes for low-velocity impact. The force versus displacement curves were derived and analyzed for each parameter variations and detailed comprehension of deformation pattern and energy absorption are provided. The objectives of the present work is to showcase the effect of honeycomb geometric parameters like thickness and cell size on crashworthiness parameters for low-velocity impact and also to represent the effect of sandwich honeycomb and honeycomb with V-Notch triggers methodology on the crashworthiness parameters like initial peak force (IPF), energy absorption (EA), specific energy absorption (SEA) and crush force efficiency (CFE)

Keywords: Crashworthiness, crash box, aluminum honeycomb, V-Notch triggers and energy absorption.

1. Introduction

Mass reduction” is one of the present challenges, being addressed by automotive design engineers. The state-of-the art materials are required for enhancing the fuel economy of contemporary automobiles along with safety, comfort and vehicle performance. As less energy is consumed to expedite a lighter object compared to heavier one, the use of light-weight materials for construction is highly recommended to upgrade vehicle performance and efficiency. This has led the automotive structural engineers to use thin sheets of metals for automobile parts which absorb less energy during crash analysis. In this aspect,

honeycomb materials are one of the most commonly employed lightweight materials in the modern automotive structures. A honeycomb material offers less density and comparative high compression and shear properties. Since the honeycomb structures have high strength and stiffness-to-weight ratio, it is vastly used in lightweight structures.

Ref. [1] investigated the impact behaviour of foam-filled honeycomb sandwich panels and compared it to the unfilled honeycomb panels and circular tubes. It was concluded that foam filled honeycomb structure have a promising result for impact loads compared to unfilled honeycomb. Here, the energy absorption is always related to the impact energy and the foam filled honeycomb diminishes the

peak compressive force and increases the specific absorbed efficiency. The honeycomb structures have a fair strength to weight ratio and can replace metal alloys in automobile crash-worthiness scenarios such as bumper and crash boxes.

Crash box plays an important role in absorbing the impact energy in case of a frontal impact. [2] studied the deformation performance of reinforced hexagonal honeycomb. The model parameters considered for optimization were stiffener thickness, expanding angle, cell length, wall thickness, constraint, impact mass and impact speed. It was concluded that peak stress increases with stiffener thickness and expanding angle has no adverse effect on the peak stress of the reinforced hexagonal honeycomb. [3] concluded that aluminum honeycombs in association with polymeric foams exhibits supercilious energy absorption characteristics as compared to expanded polystyrene foams under quasi-static and dynamic loading conditions. Here, the energy absorption increases with the thickness of the honeycomb layer, the density of the foam and the loading speed.

[4] investigated functionally graded honeycomb in square section crash columns with oblique loading for performance in crash-worthiness. The outcome of the research revealed that the functionally graded honeycomb filled crash box structures surpassed the uniform honeycomb filled crash box columns in terms of performance. [5] reported that honeycombs filled with square tubes show a unique mechanical behavior. The study also projected that if the cellular honeycomb is used as refill, the resulting composite structure have a higher initial peak force at the buckling stage, showcases a nearly constant strength acceleration at the plateau stage, and guides to quicker densification stage. These are favorable conditions for better load-carrying capacity and escalating the energy absorption. [6] studied the response of a honeycomb core to an axial quasi-static compressive force with displacement control for various cell wall thicknesses and sizes. It was concluded that decreasing the cell size and increasing the cell wall thickness resulted in the improved compressive strength of the honeycomb core. [7] studied the vehicle-barrier impact for various configurations of chassis front rails for proper combination. The goal of the analysis was to study the plastic deformation and to increase energy absorption by the chassis front rails of the automotive structure and to increase vehicle crash time for more safety of vehicle occupants. It was concluded that the configurations like the added bumper beam escalated the impact energy absorption and transferred the impact energy to the bumper by which

it reduced the impact load to the main chassis and the occupants.

[8] examined the crash-worthiness capability of aluminum hexagonal honeycomb structures under impact loads. The physical parameters like aluminum foil thickness, cell size, cell progression angle, impact velocity and mass were accounted for numerical analysis with the dynamic behavior and the crashworthiness parameters were analysed. From numerical investigations, it was proved that crash-worthiness parameters had a conditional effect on cell dimensions and foil thickness of the honeycomb core but displayed no influence on varying impact mass and velocity. [9] inspected the paper honeycomb structure for dynamic loading under medium and low strain rates and reported a significant difference in mechanical properties between dynamic and static loading conditions. The analytical model designed by [10] predicted the crushing strength and stress at the supporting ends as a function of impact speed, base material physical properties, cell size and cell wall angle. It was showcased as that the honeycomb's crushing strength will improve and supporting stress could diminish with the increase of impact velocity. The analytical equation of the critical velocity was derived, which offers the functions of the honeycomb's crushing strength for low-velocity and high-velocity impacts.

[11] explored the deformation of square packed and hexagonal packed circular-celled honeycombs for dynamic out-of-plane impact loading. It was found that the energy absorption per unit mass of the hexagonal packed honeycomb was 13.3 % greater and the square packed honeycomb was also 6.4% greater than that of the nominal cylindrical tubes. [12] investigated a double honeycomb sandwich panel where the transverse position rather than the middle of the intermediate face sheet was changed. The effect of the transverse position was numerically studied with a point-based internal-structure model and a material-point method. It was found that a superior shielding performance can be attained when the distance between the intermediate face sheet and the front face sheet is around the equivalent shielding distance. [13] scrutinized the velocity perceptive of aluminum honeycomb for high-speed axial impact (20 to 80 m/s). The major outcome was the plateau stress accelerates for the impact speed of 30 m/s, but progresses for the velocity range of 30 to 80 m/s. It was showcased that the energy-absorbing capability escalates with the impact velocity and the honeycomb core density. [14] investigated glass-fiber reinforced polyamide honeycomb embedded in a hollow steel tube. It was concluded that the peak load was truncated by 37% on a specimen with similar mass

and the specific energy absorbed was improved by 39.5% for the same specimen compared to that of unfilled one.

Even though many analytical and numerical investigations were performed on various honeycomb cores for static, dynamic and high-speed loading conditions as cited by the above literature [1-14], the effect of crashworthiness parameters with respect to honeycomb physical parameters like honeycomb cell size and its foil thickness when used as filler to the base material has not been investigated to a great extent.

Honeycomb cores have become popular in the automotive sector because of its light weight and good energy absorbing characteristics. However, the effect of variations in cell size and its geometry on the crashworthiness parameters when embedded with HSS crash boxes has not been studied in detail earlier.

More over, the benefits of cross sectional arrangement and buckling initiators (geometrical features introduced to benefit out the required crushing deformation and performance) has also not been investigated in detail. One of the key feature of HSS is the tendency of positive strain rate. In general, higher strain rates are noticed at crashworthiness occasions (strain rates can shoot up to 500 s⁻¹). Inevitably, the coalition of strength, rapid strain hardening characteristics, ductility, sensitiveness to strain-rate and formability of HSS materials proves its higher capacity of energy absorption during crash analysis, than conventional low carbon steels or structural components made of aluminium[17].

In the current research, the crash-worthiness characteristics of a crash box made of HSS material filled with aluminium honeycomb is analysed with various types of geometrical parameters and trigger configurations. A further study has been performed by introducing reinforced sandwich honeycomb with steel plates in to HSS crashbox. In addition to this, the analysis is also carried out by inducing fold initiators like V-Notch triggers in the honeycomb core to check the effect of crashworthiness parameters. A comparative numerical interpretation was performed to explore the performance of initial peak force, energy absorption, specific energy absorption and crush force efficiency for honeycomb embedded HSS crash boxes for low speed impact situations. The reaction force versus nodal displacement plots were analysed for all cases by providing detailed awareness of the force response during physical deformation. The intent of the work is to investigate the crashworthiness of aluminium honeycomb filled HSS crash boxes comprised of various honeycomb thickness, cell size and to showcase the crashworthiness ability of sandwich honeycomb and

notched honeycomb filled HSS crashbox for the energy absorption and crush force efficiency level.

2. Material properties

2.1. High strength steel (HSS) crash box

In the current analysis, the crash boxes made of HSS were considered. High strength steel materials are typically used for passenger-car applications such as door intrusion columns, B/C pillar reinforcements, cross-members and bumpers [18]. The material properties data for HSS crash box was considered from work done by [15]. The young's modulus of the material is considered as 203 GPa, poisson's ratio as 0.38, stress at 0.2 % plastic strain is 547 MPa and material constants σ_0 , Q1, C1 as 511 MPa, 215 MPa, 78 respectively.

2.2. Aluminium honeycomb filler

In the present study, aluminium honeycomb of type AA 3003 alloy is assessed as filler material for HSS crash box. As a lightweight structure, along with tremendous energy absorption achievement, honeycomb structures play a crucial role in many applications of advanced aerospace components, packaging, military devices, vehicle components etc. The hexagonal honeycombs cells are highly favored in the automotive industry usage [19]. The material properties data for honeycomb filler was considered from work done by [20]. The young's modulus is considered as 69.0 GPa, initial yield stress as 115.8 MPa, the ultimate stress as 154.5 MPa and Poisson's ratio as 0.33.

3. Numerical analysis and methodology

In the current numerical analysis, the finite element model of HSS crash box and aluminium honeycomb is modelled with Belytschko-Tsay uniform reduced shell integration rule, hourglass prevention as stiffness method using elastic modulus and strain rate as Cowper-Symonds model. The commercial finite element meshing tool Visual Mesh from ESI-GROUP is used to mesh both the crash box and honeycomb component. The finite element mesh is maintained on an average size of 8 mm for HSS crash box as shown

in Figure 1. The finite element mesh is retained as 6 mm x 2 mm along the cell size and 1.6 mm x 1.6 mm at the cell edges to maintain the proper connectivity of honeycomb as shown in figure 2. The commercial preprocessor Visual Crash-PAM from

ESI-GROUP is used for model setup and Visual-Viewer post processor was employed to analyze and interpret the output results. The elastic plastic iterative hill material algorithm supplied by PAMCRASH finite element explicit code from ESI-GROUP is used for HSS crash box and Aluminium honeycomb. A tied contact has been defined between the honeycomb and HSS crash box. All the bottom nodes of the HSS and honeycomb is defined with a boundary condition with all the translation and rotational degrees of freedom as fixed. A stationary mass of 800 Kg is defined on the moving plate which is impacted at a velocity of 32 Km/h. The output request has been defined cog node of the rigid body to record the displacements and the reaction force.

The experimental set-up was analyzed for the low speed impact test. The motivation of this test is to find the crash-worthiness of front structure crashbox of the vehicle for low speed impact (32 km/h). As per the vehicle regulation test, no component fixed behind the crashbox should found to be buckled or badly deformed during frontal crash analysis, so that there should be a very minimal destruction and remanufacturing cost. In this scenario, the crash box should progressively deform and maximum impact energy should be absorbed and very minimum force should be transferred to the vehicle cabin area. In this research, the component level study and analysis of the crash box was done in order to identify the best specifications of the geometric parameters and positioning arrangements for the Aluminum honeycomb filled HSS crashbox. The component level analysis is helpful in decision making for the current methodology and same can be adapted for the full vehicle level and other respective domains based on the analysis results. Energy absorption (EA) is a

key crashworthiness parameter to analyze crashworthiness of the component. It is defined as the area under force-displacement curve or the maximum absorbed internal energy of the component, so if more energy absorption is observed, it means that the component can absorb more energy which is a desirable condition in the automobile industry. Analytically this constant was calculated using the Eq. (1).

$$EA(d) = \int F(\delta) d\delta \quad (1)$$

Where, 'd' is crush length and 'δ' is displacement respectively and 'F' is the crushing load.

The mean crush force (Pm) was defined as the ratio between the energy absorption (EA) and the maximum displacement δ as shown in Eq. (2).

$$P_m = EA / \delta \quad (2)$$

The mean crush force (Pm) determines the total capacity of energy absorption of a structure. The balanced total energy absorption by mass is required to examine the geometry and material discrepancy in the test specimens and it is pursued by specific energy absorption SEA. The greater the SEA value indicates that the crash box can become lighter. The specific energy absorption (SEA) was determined by Eq. (3).

$$SEA = EA / m \quad (3)$$

Where, 'm' is the mass of the specimen. A higher SEA leads to a better energy absorption capacity of crash box with respect to the mass.

Crush force efficiency (CFE) is defined as the ratio between the mean crushing force and the maximum peak force [16] and was calculated using the Eq. (4).

$$CFE = P_m / P_{max} \times 100 \% \quad (4)$$

Where, 'Pm' and 'P max' are the mean crushing force and peak force respectively.

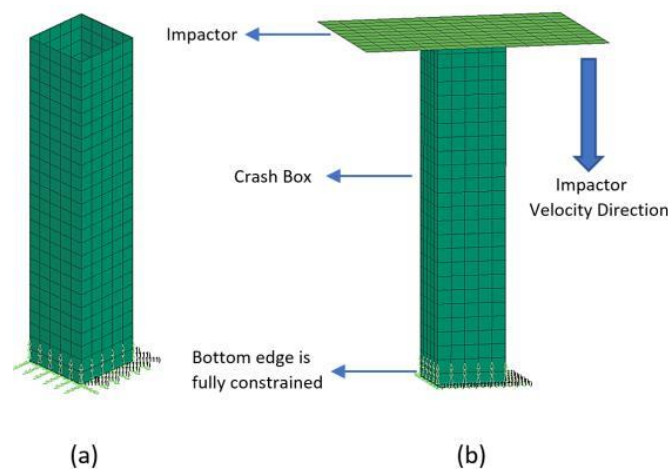


Fig1. (a) Finite element model of crash box (b) Crashbox simulation setup

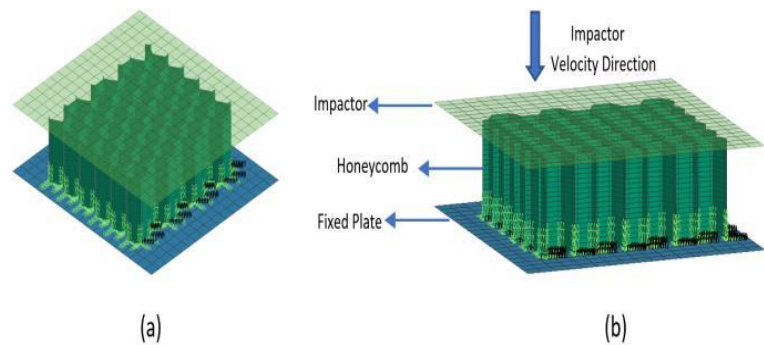


Fig2.(a) Finite element model of honeycomb (b) Impact analysis of honeycomb simulation setup.

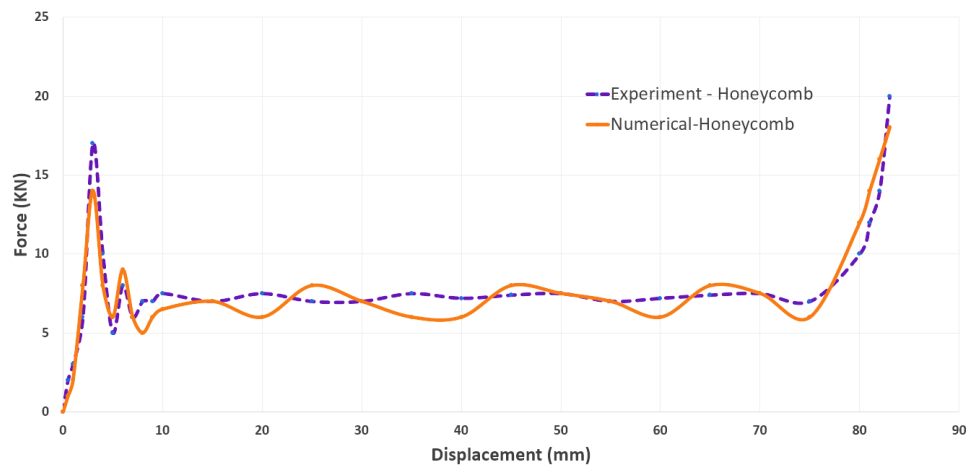


Fig3.Comparison of experiment [15] and simulation force-displacement curves for HSS material.

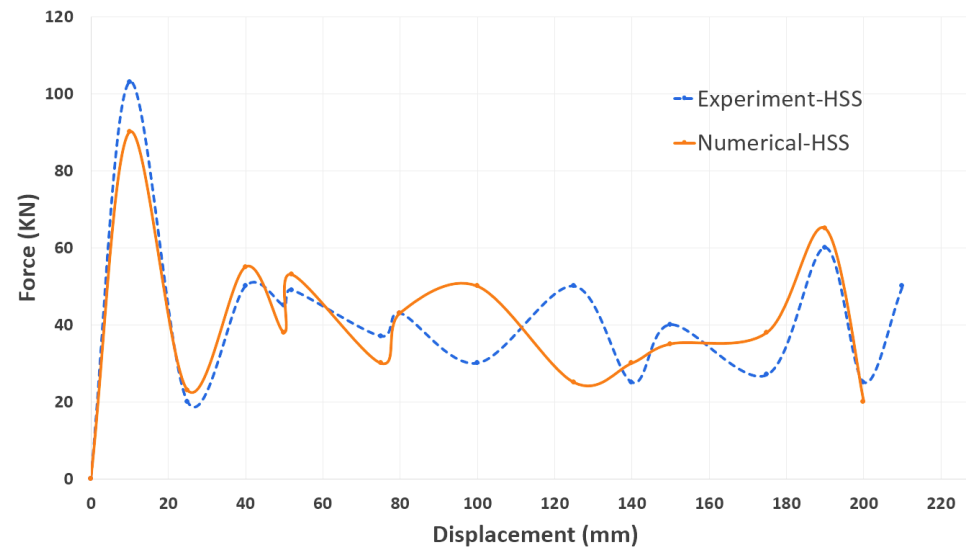


Fig4.Comparison of experiment [20] and simulation force-displacement curves for AA3003 material.

Fig5.

Table 1. Force values comparison between simulation and experiment [15] for HSS crash box

Parameter	Experiment	Simulation
Peak Force	(KN)	103 95.0
Mean Force	(KN)	40.9 39.5

Table 2. Force parameter comparison between simulation and experiment [20] for honeycomb core.

Parameter	Experiment	Simulation
Peak Force	(KN)	17 14
Mean Force	(KN)	7.8 7.6

Results and discussion

For primary authentication of HSS material properties and finite element simulation model, a correlation was performed by comparing experimental data [15] and finite element results obtained by finite element simulation in the current study. The experimental data was considered only for comparison and correlation purpose. The finite element analysis was performed in a similar way as described in the experiments conducted by [15]. For the reason of equivalence, the finite element model was built to replicate the experimental specimen, with dimensions of the HSS tube specimen as 311 mm length, cross section as 59.7 X 56.8 mm, corner radius of 3mm and thickness 1.17 mm with an impact velocity of 5 m/s.

Comparison of the test result with the finite element simulation for axial force versus displacement curves was performed (figure 3). Comparison of force parameter between simulation and experimental result was showcased in Table 1. A significant correlation was evidenced between experimental results and finite element simulation outputs. Also, the deformation modes of finite element analysis are found to be similar to that of the experimentation behavior for the given loading condition. In a similar fashion to validate the AA3003 alloy (aluminum honeycomb), a correlation analysis was performed by comparing experimental data [20] and the finite element analysis of the current study. The finite element analysis was carried out in the same way as described in the experiments conducted by [20]. For the reason of equivalence, the length of the specimen is considered as 100 mm and the cross section as 42 X 42 mm for a cell size of 6 mm for the finite element model. The axial impact velocity is maintained as 0.5 mm/s. The comparison of the test

and finite element simulation was done based on axial force versus displacement curves (figure 4) and the force parameters were interpreted with force versus displacement data and relevant magnitude was showcased in Table 2. A good correlation was observed between experimental results and finite element simulation outputs.

From figure 3 and table 1, it can be ascertained for HSS crash box that the deformation behavior and the pattern of the force versus displacement curve of the finite element simulation is in significant agreement with the experimental data. Only a moderate difference is evidenced for the force and mean force values between tests and simulation. Both the experimental and simulation curves showed a similar trend in the resistance to the deformation in the initial stage, due to which the rise in the force level was observed which is termed as (initial peak force). The structure further counters the deformation because of which a secondary peak force and so on, was observed from the force versus displacement curve. However, for the aluminum honeycomb material AA3003 (see figure 4), the force-displacement curve shows no resistance to deformation as demonstrated by the lack of peaks observed after the secondary peak force. This behavior can be explained as follows a large initial deformation occurs initially and then the structure progressively deforms by application of the load. At this junction, the folding initiators play a key role and are a matter of great interest for smooth energy absorption. The V-Notched triggers can initiate the folding locally in that region and then the structure can progressively deform in a regular manner than deforming abruptly. In these types of situations, the use of V-Notch triggers provides a secondary peak force, which helps to intensify the energy absorption, which is preferable in high-speed impact analysis. Earlier reports [21,22] concluded that honeycomb filled cashbox exhibits better energy

absorption and desirable deformation modes and in the current, research the effect of cell size and thickness of the honeycomb is studied and analyzed for the effect of the crashworthiness parameters. In addition, a numerical analysis has been carried out by reinforcing the sandwich honeycomb separated by steel plates in HSS cashbox. [23] Studied the impact of triggers in axial impact analysis and in the current study, a novel method of instigating a notch trigger in an aluminum honeycomb is studied and analyzed.

The height of HSS boxes is maintained as 273 mm and wall thickness as 2 mm for the entire study. The cross-section geometry of HSS crash box is illustrated in Figure 5. The authenticated simulation model setup was adopted for HSS crash box and aluminum honeycomb study; the material properties were kept unchanged and only the geometry of the HSS crash boxes and aluminum honeycomb was changed as per the cases required for the current study.

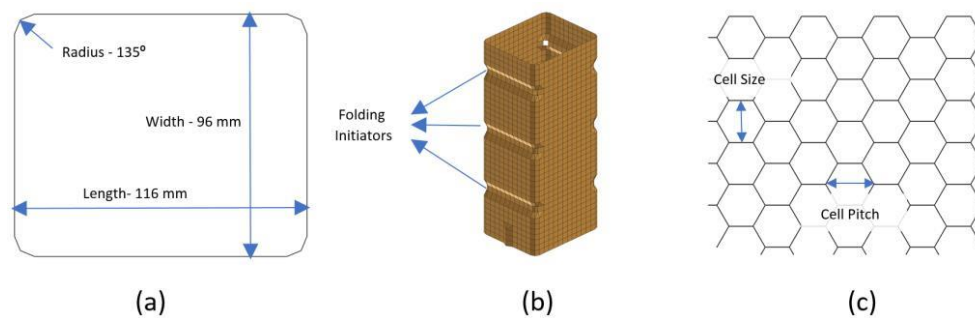


Fig6. (a) 2D Dimensions of HSS crashbox (b) HSS crashbox with folding initiators. (c) 2D representation of honeycomb for cell size and cell pitch

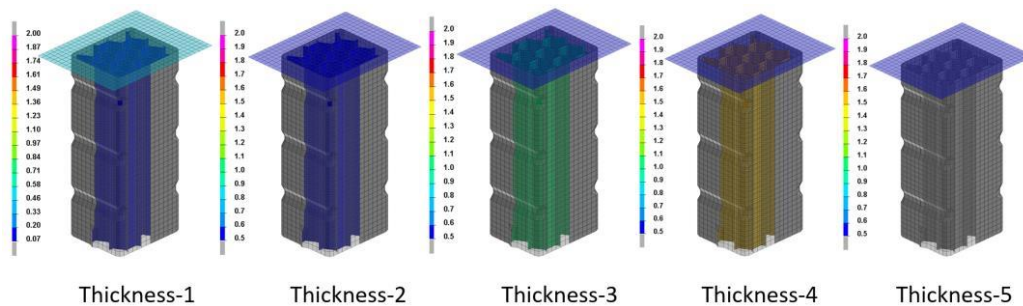


Fig7. Thickness contour of HSS filled with Honeycomb of various thickness before impact test

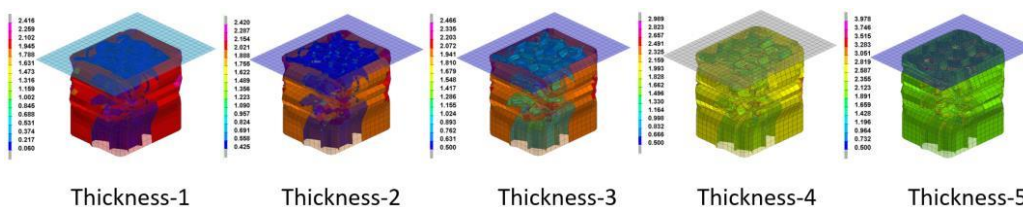


Fig8. Thickness contour of HSS filled with Honeycomb of various thickness after impact test

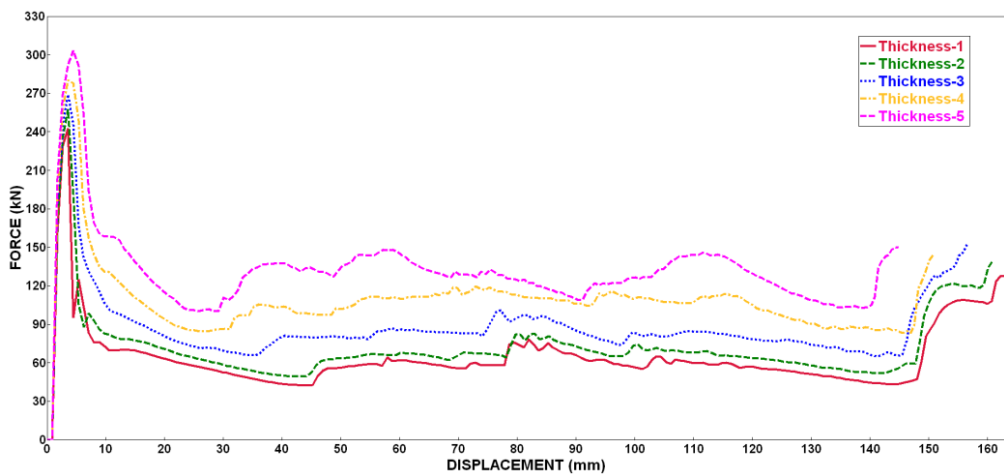


Fig9. Force-displacement curves of HSS crash box filled with honeycomb of various thickness

Table 3. Crashworthiness parameters of HSS crash box filled with honeycomb of various thicknesses

S. No	Sample	Thickness (mm)	Mass (Kg)	IPF (KN)	Mean Force (KN)	EA (KJ)	SEA (KJ/Kg)	CFE
1	Thickness Variation-1	0.07	1.7	242.6	64.56	10.1	5.71	26.6
2	Thickness Variation-2	0.5	1.9	257.6	72.36	11.5	5.85	28.0
3	Thickness Variation-3	1	2.2	269.0	87.89	13.6	6.22	32.6
4	Thickness Variation-4	1.5	2.4	280.0	108.6	16.2	6.70	38.8
5	Thickness Variation-5	2.0	2.6	303.5	129.1	17.9	6.76	42.5

4.1. Variation of honeycomb thickness

The finite element method was adopted for varying thickness of honeycomb without changing the geometry and physical parameters of the HSS crash box. Honeycomb thickness dimensions are varied as 0.07 mm, 0.5 mm, 1 mm, 1.5 mm and 2 mm, based on the exposition of the thickness, and the samples are denoted as Thickness-1, Thickness-2, Thickness-3, Thickness-4 and Thickness-5 (see Figures 6 and 7) respectively. All the five types of crash boxes are crushed by a rigid impactor with a fixed mass of 800 kg at axial velocity of 32 kmph as shown in Figure 1. From the force-displacement plots of HSS crash box filled with honeycomb of various thickness variations (Figure 8) and the crashworthiness parameters values (from Table 3). It can be perceived that the thickness variation-5 has the maximum energy absorption (EA), specific energy absorption (SEA) and crush force

efficiency (CFE) compared to all other samples with 17.97 KJ, 6.76 KJ/KG and 42.53 respectively. The energy absorption (EA), specific energy absorption (SEA) and crush force efficiency (CFE) is lowest for thickness variation-1 specimen with values of 10.17 (KJ), 5.71 (KJ/KG) and 26.61 respectively. The EA is a predominant factor which decides the crash worthiness ability of a component and the SEA is another important constant to evaluate the energy absorption with respect to mass of the crushing component. CFE is the variable which illustrates the uniformity of collapse force.

Lower the values of CFE and higher the peak force results in an increase in non-uniform acceleration and CFE potential damage to the occupants during frontal impact analysis which is undesirable. The results (Figure8) illustrate that there is a conspicuous improvement in initial peak force level for thickness variation-5 sample due to which

the energy absorption is also augmented, as this phenomenon increases the area under the force displacement curve. A good response of SEA and

CFE is exhibited by the similar trend the SEA and CFE exhibited good response and high in magnitude for thickness variation -5 sample.

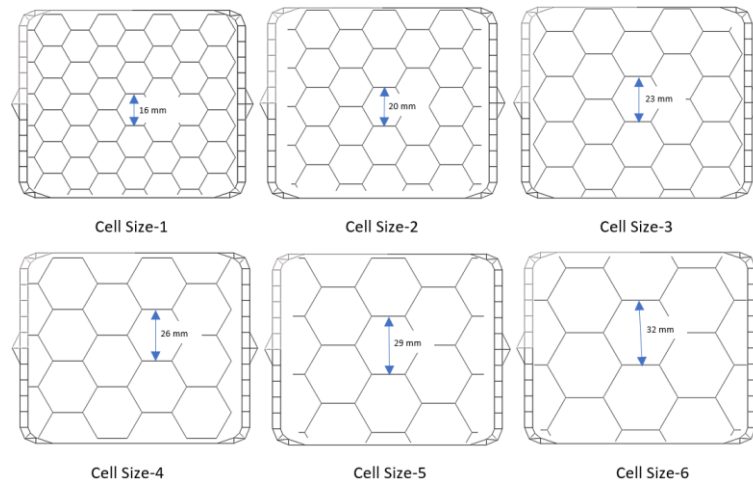


Fig10. Top view of HSS filled with Honeycomb of various cell size before impact test

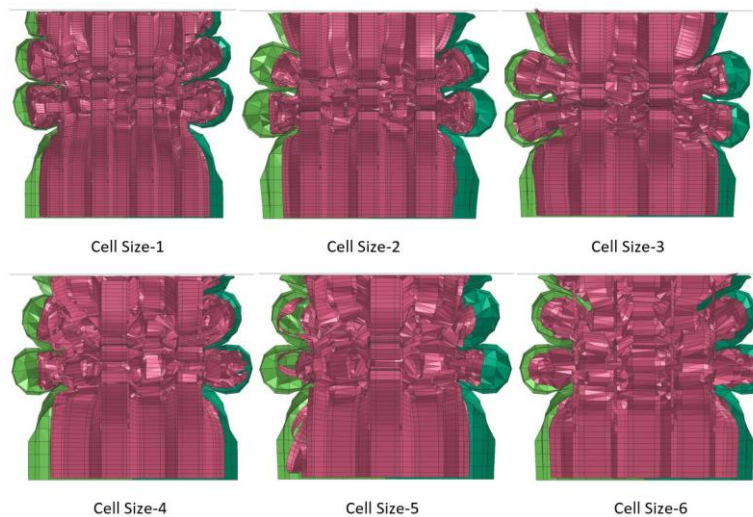


Fig11. Section view of HSS filled with Honeycomb of various cell size after impact test.

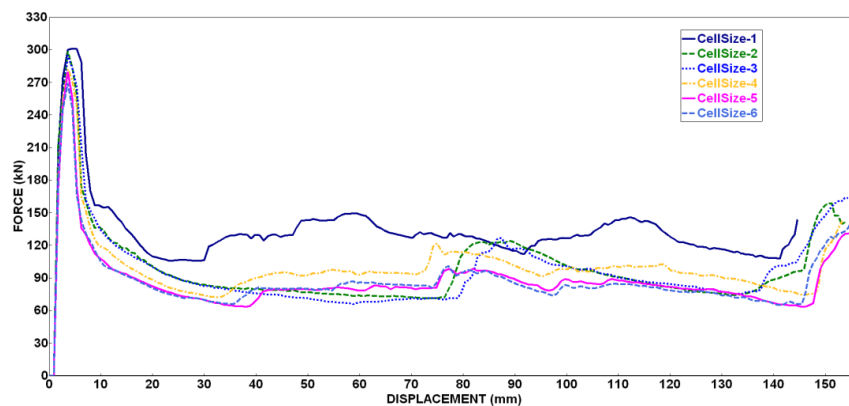


Fig12. Force-displacement curves of HSS crash box filled with honeycomb of various cell sizes.

Table 4. Crashworthiness parameters of HSS crash box filled with honeycomb with various Cell Size

S. No	Sample	Cell Size (mm)	Mass (Kg)	IPF (KN)	Mean Force (KN)	EA (KJ)	SEA (KJ/Kg)	CFE
1	Cell Size-1	16	2.67	301.13	128.78	18.11	6.78	42.77
2	Cell Size-2	20	2.44	298.15	98.33	15.01	6.15	32.98
3	Cell Size-3	23	2.42	295.11	97.03	14.91	6.16	32.88
4	Cell Size-4	26	2.32	282.17	90.06	13.93	6.00	31.91
5	Cell Size-5	29	2.21	279.44	87.89	12.69	5.74	31.45
6	Cell Size-6	32	2.20	269.06	83.28	12.02	5.46	30.95

4.2. Variation of honeycomb cell size

Finite element method was adopted for different cell sizes of honeycomb without changing the geometry and physical parameters of HSS crash box. Honeycomb cell size dimensions are varied as 16 mm, 20 mm, 23 mm, 26 mm, 29 mm and 32 mm, based on the exposition of the cell size, the samples are named as Cell Size-1, Cell Size-2, Cell Size-3, Cell Size-4, Cell Size-5 and Cell Size-6 (Figure 9) respectively. All the six types of crash boxes are crushed with a rigid impactor with a fixed mass of 800 kg at axial velocity of 32 kmph as represented in Figure 1. The results of the force-displacement plots of HSS crash box filled with honeycomb of various cell size variations (Figure 11) and the crashworthiness parameters values (Table 4), demonstrate that the cell size-1 has the maximum energy absorption (EA), specific energy absorption (SEA) and crush force efficiency (CFE) compared to all other samples with 18.11 KJ, 6.78 KJ/Kg and 42.77 respectively. The energy absorption (EA), specific energy absorption (SEA) and crush force efficiency (CFE) is lowest for cell size-6 specimen with values of 12.02 KJ, 5.46 KJ/Kg and 30.95 respectively. From figure 10, it can be observed that for Cell Size-1, the deformation modes of HSS and AA3003 aluminium honeycomb are in the same phase. As the honeycomb cell size is minimum, all the cells can deform uniformly along with HSS box to replicate the same folding patterns. This phenomenon helps the component for uniform folding and maximum compression which results in a higher energy absorption. EA, SEA and CFE are the predominant factors which decides crashworthiness ability of a component. It is CFE illustrated from the above results (Figure 11) that there is a significant enhancement in the initial peak force level for cell

size-1 sample which is the desired behaviour for SEA. The CFE is increased because of increase in energy absorption.

4.3. Impact analysis of HSS filled with sandwich honeycomb

Finite element method was employed to analyze HSS crashbox filled with sandwich honeycomb. From the Table 3 and Figure 8, it is observed that a honeycomb thickness of 2 mm showed desirable results. Hence, the honeycomb thickness for this study was considered as 2 mm and cell size as 32 mm. A steel plate of 2 mm thickness is used to separate the honeycomb in to five pieces to form a honeycomb -steel plate sandwich structure. The HSS crash box, filled with sandwich honeycomb was impacted with a rigid impactor with a rigid mass of 800 kg at an axial velocity of 32 kmph as represented in Figure 12. The output of this analysis was compared with a HSS crash box filled with regular honeycomb. From the force displacement plots of HSS crash box filled With sandwich honeycomb (Figure 13) and the crashworthiness parameters values (Table 5), it is perceived that the HSS crash box filled with sandwich honeycomb showed unsatisfactory results with minimum energy absorption (EA), specific energy absorption (SEA) and crush force efficiency (CFE) compared to HSS crash box filled with regular honeycomb with 16.93 KJ, 5.08 KJ/KG and 41.40 respectively. It can be concluded that (Figure 13) there was a conspicuous diminution in the initial peak force for of HSS crash box filled with sandwich honeycomb sample due to which the energy absorption is also diminished. The SEA and CFE parameters also show undesirable results indicating that the sandwich phenomenon is not recommended for impact load cases.

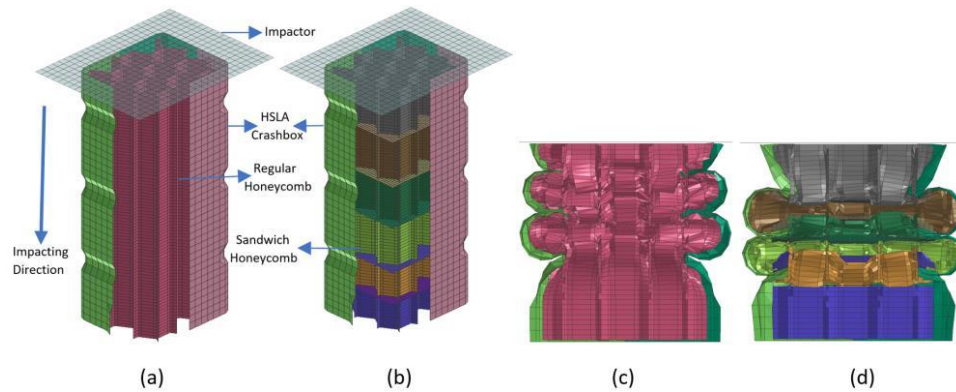


Fig13. (a) HSS filled with regular honeycomb before impact. (b) HSS filled with sandwich honeycomb before impact. (c) HSS filled with regular honeycomb after impact. (d) HSS filled with sandwich honeycomb after impact.

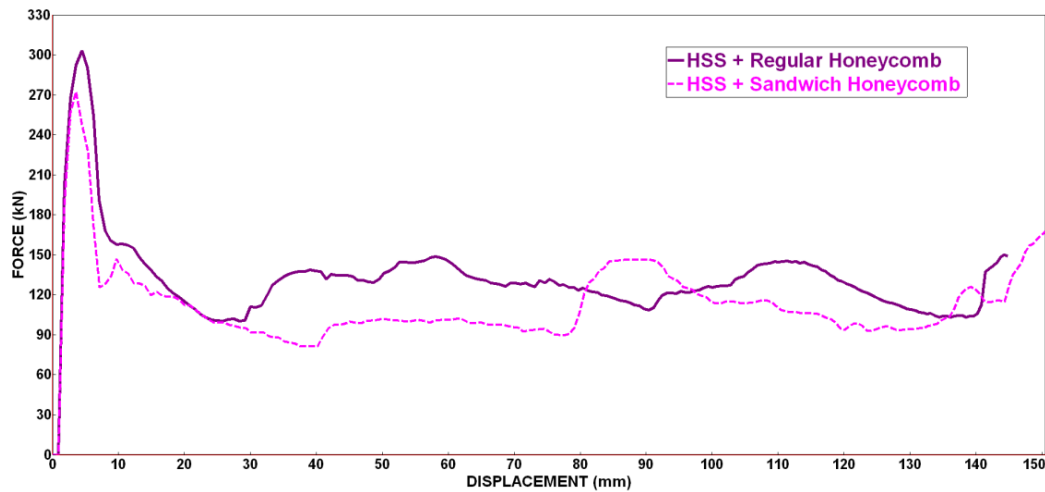


Fig14. Force-displacement curves of HSS crash box filled with regular honeycomb and sandwich honeycomb

Table 5. Crashworthiness parameters of HSS crashbox filled with with regular honeycomb and sandwich honeycomb.

S. No	Sample	Mass (Kg)	IPF (KN)	Mean Force (KN)	EA (KJ)	SEA (KJ/Kg)	CFE
1	HSS + Regular Honeycomb	2.66	303.53	129.09	17.9	6.76	42.53
2	HSS+ Sandwich Honeycomb	3.33	273.14	113.07	16.9	5.08	41.40

4.4. Impact analysis of HSS filled with V-Notched honeycomb.

Finite element method was adopted to analyze HSS crashbox filled with V-Notched honeycomb. The honeycomb thickness for this study was considered as 2 mm and cell size as 32 mm. The HSS crash box filled with V-Notched honeycomb was

impacted with a moving impactor with a rigid mass of 800 kg at axial velocity of 32 kmph as represented in Figure 14. The V- Notch was introduced with an angle of 90° on all the outer edges of the honeycomb core and with a distance of 83.5 mm each other as shown in figure 16.

The V-Notch triggers are in parallel with the fold initiators of HSS crashbox. This arrangement is to

avail the advantage of synchronized folding of aluminum honeycomb and HSS crash box in a same plane and in a same mode. The output results of HSS crash box filled with notched honeycomb was compared with a HSS crash box filled with regular honeycomb. From the force-displacement plots of HSS crash box filled with notched honeycomb (Figure 17) and the crashworthiness parameters values (Table 6), it can be perceived that HSS crash box filled with notched honeycomb showed satisfactory results with better energy absorption

(EA), specific energy absorption (SEA) and crush force efficiency (CFE) with 19.74 KJ, 7.89 KJ/KG and 44.02 respectively. The above results (table 6) illustrate a moderate increase in CFE with a considerable increase in EA and SEA values when the total mass of the structure is reduced marginally. Decreasing the mass and increasing the performance of the component is the most favorable condition for enhancing the crashworthiness. Hence the V-Notched honeycomb structure unveils a significant advantage over the regular honeycomb.

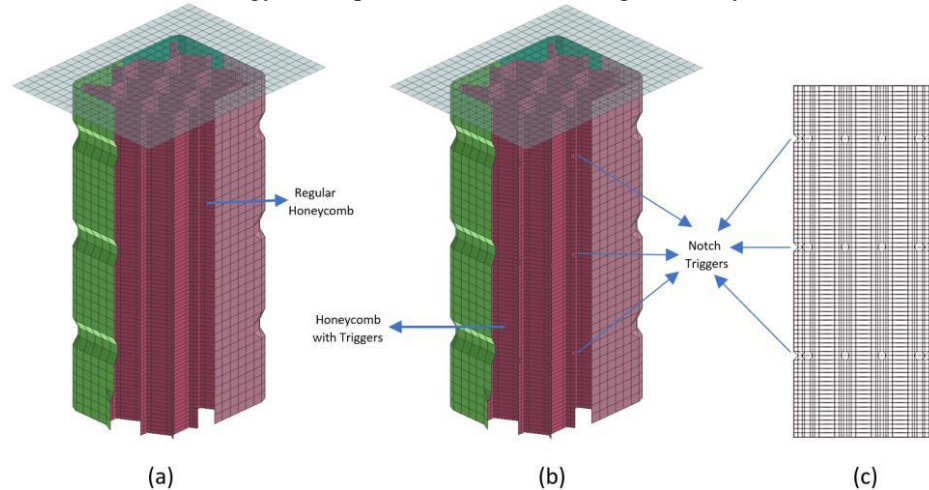


Fig15. (a) HSS filled with regular honeycomb before impact. (b) HSS filled with V-Notched honeycomb before impact. (c) 2D wireframe view of honeycomb with V-Notch triggers before impact

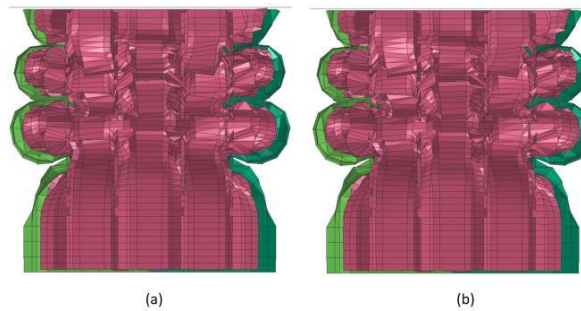


Fig16. Deformation modes of (a) HSS filled with regular honeycomb after impact. (b) HSS filled with VNotch triggered honeycomb after impact.

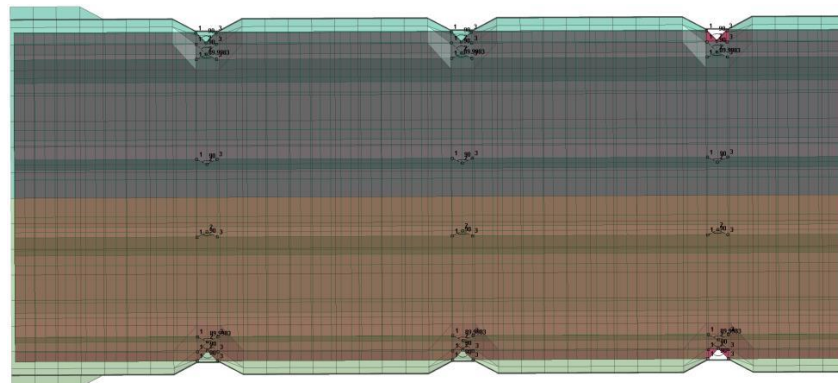


Fig17. Showing 900 V-Notch in honeycomb parallel to the folding initiators of HSS crashbox

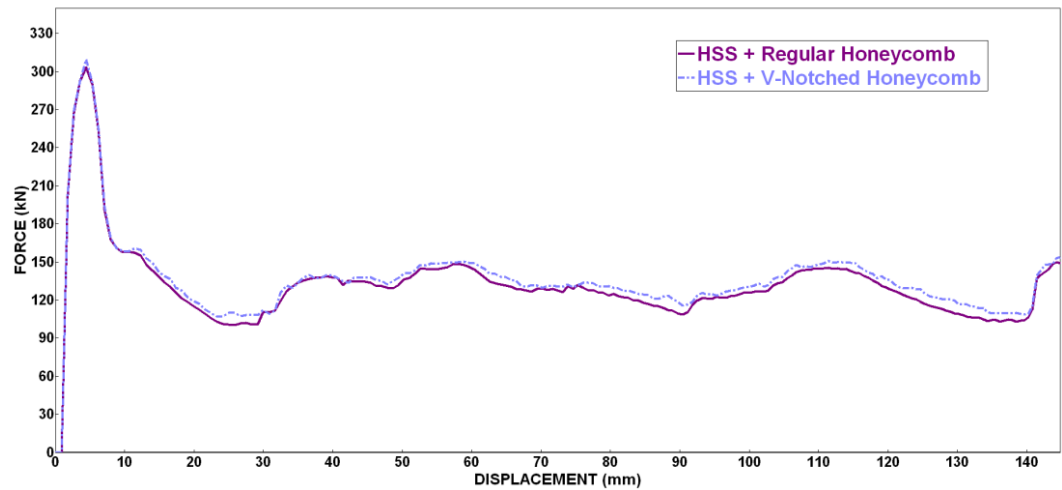


Fig18. Force-displacement curves of HSS crash box filled with regular honeycomb and V-Notched honeycomb.

Table 6. Crashworthiness parameters of HSS crashbox filled with regular honeycomb and V-Notched honeycomb

S. No	Sample	Mass (Kg)	IPF (KN)	Mean Force (KN)	EA (KJ)	SEA (KJ/Kg)	CFE
1	HSS + Regular Honeycomb	2.66	303.53	129.09	17.9	6.76	42.53
2	HSS+V-Notched Honeycomb	2.50	309.68	136.31	19.7	7.89	44.02

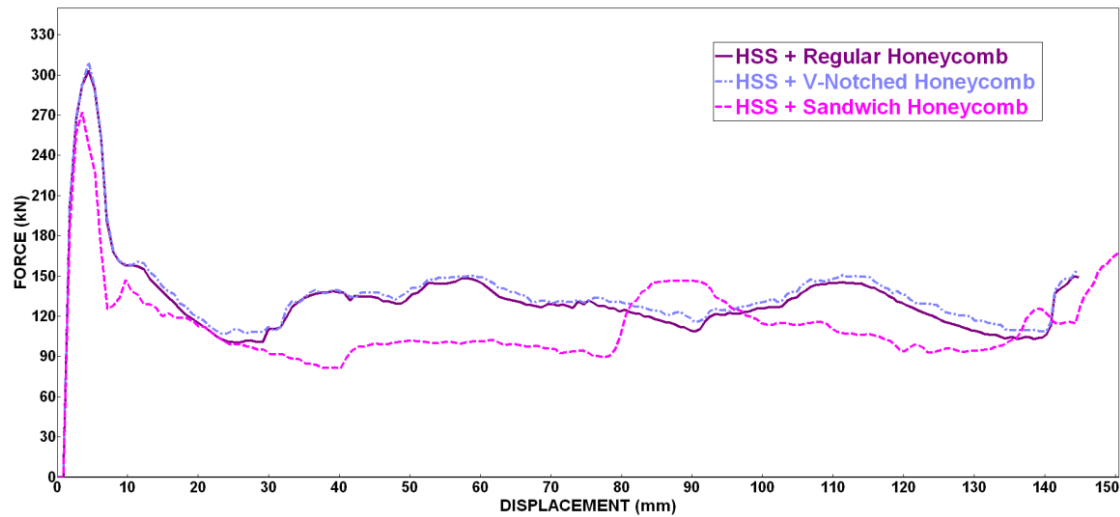


Fig19. Force-displacement curves of HSS crash box filled with regular honeycomb, sandwich honeycomb and V-Notched honeycomb

Table 7. Crashworthiness parameters of HSS crashbox filled with regular honeycomb sandwich honeycomb and V-Notched honeycomb.

S. No	Sample	Mass (Kg)	IPF (KN)	Mean Force (KN)	EA (KJ)	SEA (KJ/Kg)	CFE
1	HSS + Regular Honeycomb	2.66	303.53	129.09	17.97	6.76	42.53
2	HSS+ Sandwich Honeycomb	3.33	273.14	113.07	16.93	5.08	41.40
3	HSS+ V-Notched Honeycomb	2.50	309.68	136.31	19.74	7.89	44.02

Table 8. Crashworthiness parameters of HSS crashbox filled with thickness variation honeycomb, various cell size honeycomb, regular honeycomb, sandwich honeycomb and V-Notched honeycomb.

S. No	Sample	Thickness/Cell Size (mm)	Mass (Kg)	IPF (KN)	Mean Force (KN)	EA (KJ)	SEA (KJ/Kg)	CFE
1	Thickness Variation-1	0.07	1.78	242.66	64.56	10.17	5.71	26.61
2	Thickness Variation-2	0.5	1.97	257.65	72.36	11.52	5.85	28.08
3	Thickness Variation-3	1	2.2	269.06	87.89	13.68	6.22	32.67
4	Thickness Variation-4	1.5	2.43	280.09	108.68	16.27	6.70	38.80
5	Thickness Variation-5	2	2.66	303.53	129.09	17.97	6.76	42.53
6	Cell Size-1	16	2.67	301.13	128.78	18.11	6.78	42.77
7	Cell Size-2	20	2.44	298.15	98.33	15.01	6.15	32.98
8	Cell Size-3	23	2.42	295.11	97.03	14.91	6.16	32.88
9	Cell Size-4	26	2.32	282.17	90.06	13.93	6.00	31.91
10	Cell Size-5	29	2.21	279.44	87.89	12.69	5.74	31.45
11	Cell Size-6	32	2.20	269.06	83.28	12.02	5.46	30.95
12	HSS + Regular Honeycomb	2/32	2.66	303.53	129.09	17.97	6.76	42.53
13	HSS+ Sandwich Honeycomb	2/32	3.33	273.14	113.07	16.93	5.08	41.40
15	HSS+ V-Notched Honeycomb	2/32	2.50	309.68	136.31	19.74	7.89	44.02

4.5. Comparison of regular honeycomb with sandwich honeycomb and V-Notched honeycomb.

Numerical comparison was done between HSS filled with regular honeycomb, sandwich honeycomb and honeycomb with V-Notch triggers. The output results of HSS crash box filled with sandwich honeycomb and honeycomb with V-Notch triggers are compared with a HSS crash box filled with regular honeycomb. From the force-displacement plots (Figure 18) and the crashworthiness parameters values (Table 7), it can be perceived that HSS crash box filled with V-Notched honeycomb showed outstanding results with maximum energy absorption (EA), specific energy absorption (SEA) and crush force efficiency (CFE) with 19.74 KJ, 7.89 KJ/Kg and 44.02 respectively. It can be concluded that the superior specimen component in this numerical analysis, in terms of axial crashworthiness, was the HSS square crash box filled with VNotched

aluminium honeycomb. The initial peak force (IPF) of HSS square crash box filled with VNotched aluminium honeycomb structural components was 2% greater than the regular honeycomb and 14 % greater than the sandwich honeycomb. In a similar fashion, the energy absorption (EA) of HSS square crash box filled with V-Notched aluminium honeycomb specimen components are escalated up to 10 % more than the EA of HSS filled with regular honeycomb and 17 % more than the EA of HSS filled with sandwich honeycomb. The specific energy absorption (SEA) of the HSS square crash box filled with VNotched aluminium honeycomb follows the similar trend and is improved up to 17% more than the regular honeycomb and 55 % more than the SEA of HSS filled with sandwich honeycomb. The crush force efficiency (CFE) of the HSS square crash box filled with V-Notched aluminium honeycomb is augmented by 4 % compared to the CFE of HSS filled with regular honeycomb and by 7 % to the CFE of HSS filled with sandwich honeycomb at an axial impact velocity of 32 kmph. The deformation mode and crushing forces of HSS crash box filled with

sandwich honeycomb were found to be detrimental during low velocity impact. On the other hand, the deformation mode and crushing forces of HSS square crash box filled with V-Notched aluminium honeycomb were relatively sensitive and offers significant dominance to low impact velocities which is most desirable conditions for automotive impact analysis.

Conclusions

In this current research, the effect of physical parameters of honeycomb on crashworthiness parameters was analysed substantially when employed as fillers in HSS crash box. Further study has explored the effect of sandwich honeycomb and honeycomb with V-Notch triggers on the crashworthiness parameters when filled in HSS crash box. It was observed that the response of honeycomb filled crash boxes under impact loading changes exceptionally with physical parameters of honeycomb, modelling of honeycomb and the use of V-Notch type triggers when used for different types Of HSS crash boxes. The parameters focused in this study were energy absorption (EA), specific energy absorption (SEA) and crush force efficiency (CFE) as these parameters account for the total crashworthiness capability of the automotive structure. The aluminium honeycomb of 2mm thickness and 16mm cell size were found to be most desirable as they exhibited highest EA, SEA and CFE. When HSS filled with regular honeycomb and sandwich honeycomb are compared, HSS filled with regular honeycomb has better properties. In a similar fashion when HSS filled with regular honeycomb and honeycomb with V-Notch triggers are compared. From the values mentioned in table 8 HSS filled with V-Notch triggered honeycomb has better EA, SEA, CFE. Analyzing all the above cases, overall highest value of EA, SEA, CFE was evidenced for HSS crash box filled with V-Notch triggered honeycomb with values as 19.74 KJ, 7.89 KJ/Kg and 44.02 and the overall lowest value of EA, SEA, CFE was evidenced for HSS crash box filled with thickness variation-1 (70 microns) with values as 10.17 KJ, 5.71 KJ/KG and 26.61. From the above numerical study, it is deduced that EA of HSS filled with V-Notched honeycomb increased by 10 %, SEA increased by 17 % and CFE increased by 4 % compared to HSS filled with regular honeycomb. In addition to this, EA of HSS filled with V-Notched honeycomb increased by 17 %, SEA increased by 55 % and CFE increased by 7 % compared to HSS filled with sandwich honeycomb. Therefore, it can be concluded that

different geometric parameters of honeycomb, sandwich honeycomb and honeycomb with V-Notch triggers offer different energy absorption values. It was observed that the deformation mode was affected significantly by the geometrical parameters of honeycomb and the usage of sandwich and V-Notch triggered honeycomb.

Hence, this research has unearthed the effect of geometrical parameters like honeycomb thickness and cell size when filled with HSS crash boxes subjected to axial impact loading and has provided a comparison of the crashworthiness behaviour for all the variations. In addition to that this research explains the effect of crashworthiness parameters when HSS crash box is filled with sandwich honeycomb and V-Notch triggered honeycomb for impact loading. Thus, this study has brought out a clear picture of how the energy absorption varies for different parameters and different structural designs of honeycomb core. This study has brought out a comparative significance for usage of V-Notch triggers in the honeycomb core. This study has shown that the initial peak force magnitude, energy absorption quantity and crush force efficiency factors can be controlled and the desired crashworthiness can be achieved by adopting an appropriate honeycomb cell size, cell thickness and triggers for the respective geometrical cross section.

Hence, this study may become useful for automotive engineers dealing with composites components subjected to axial impact where the initial peak force and the deformation mode are the key factors. This study succeeded in showcasing the effects of geometrical parameters of honeycomb and triggers for crashworthiness of HSS crash boxes filled with honeycombs and to highlight the relative effect of V-Notch trigger on the total energy absorption, specific energy absorption and crush force efficiency. Thus, this study can be considered as a template for selecting the honeycomb cell thickness, cell size and V-Notch triggered honeycomb in HSS crash boxes. Hence, it can be noted that use of proper combination of geometry parameter and V-Notch trigger plays an important role in achieving desired level of energy absorption and crush force efficiency for low velocity impact conditions.

Acknowledgement

A special gratitude to ESI-GROUP for offering us the software of Visual Mesh, Visual Crash-PAM, Virtual Performance Solution and Visual Viewer for the current research and finite element analysis.

References

- [1]. Hozhabr-Mozafari., Soroush-Khatami., Habibollah-Molatefi., Vincenzo-Crupi., Gabriella-Epasto and Eugenio-Guglielmino.: Finite element analysis of foam-filled honeycomb structures under impact loading and crashworthiness design, *Int. J. Crashworthiness*, 2016.
- [2]. Qiang-He. and Da-Wei-Ma.: Parametric study and multi-objective crashworthiness optimisation of reinforced hexagonal honeycomb under dynamic loadings, *Int. J. Crashworthiness*, 2015.
- [3]. Caserta, G., Galvanetto, U. and Iannucci, L.: Static and Dynamic Energy Absorption of Aluminum Honeycombs and Polymeric Foams Composites, *Mechanics of Advanced Materials and Structures*, (17), 2010, 366-376.
- [4]. Mohammadiha, O., Beheshti, H. and Haji-Aboutalebi, H.: Multi-objective optimisation of functionally graded honeycomb filled crash boxes under oblique impact loading, *Int. J. Crashworthiness*, 20(1), 2015, 44-59.
- [5]. Zhonggang-Wang., Shuguang-Yao., Zhaijun-Lu., David-Hui. and Luciano-Feo: Matching Effect of Honeycomb-filled Thin-Walled Square Tube -Experiment and Simulation, *Composite Structures*, 2016.
- [6]. Khoshravan, M.R. and Najafi Pour, M.: Numerical and experimental analyses of the effect of different geometrical modelings on predicting compressive strength of honeycomb core, *Thin-Walled Structures*, 84(1), 2014, 423-431.
- [7]. Ali Balaei Sahzabi1, Mohsen Esfahanian1.: The Effects of Thin-Walled Structure on Vehicle Occupant's Safety and Vehicle Crashworthiness, *International Journal of Automotive Engineering*, 7(2), 2017, 2393-2403.
- [8]. Ahmad-Partovi-Meran., Tuncer-Toprak., Ata-Mugan.: Numerical and experimental study of crashworthiness parameters of honeycomb structures, *Thin-Walled Structures*, 78(1), 2014, 87-94.
- [9]. Wang-Dongmei. and Bai-Ziyu.: Mechanical property of paper honeycomb structure under dynamic compression, *Materials and Design*, 77(1), 2015, 59-64.
- [10]. Hu, L. L. and Yu, T.X.: Mechanical behavior of hexagonal honeycombs under low-velocity impact –theory and simulations, *International Journal of Solids and Structures*, 50(1), 2013, 3152-3165.
- [11]. Hu, L. L., He, X. L., Wu, G. P. and Yu, T. X.: Dynamic crushing of the circular-celled honeycombs under out-of-plane impact, *International Journal of Impact Engineering*, 75(1), 2015, 150-161.
- [12]. Ping-Liu., Yan-Liu., and Xiong-Zhang.: Improved shielding structure with double honeycomb cores for hyper-velocity impact, *Mechanics Research Communications*, 69(1), 2015, 34-39.
- [13]. Zhonggang-Wang., Hongqi-Tian., Zhaijun-Lu. and Wei-Zhou.: High-speed axial impact of aluminum honeycomb – Experiments and simulations, *Composites: Part B*, 56(1), 2014, 1-8.
- [14]. Paz, J., Diaz, J., Romera, L. and Costas, M.: Crushing analysis and multi-objective crashworthiness optimization of GFRP honeycomb-filled energy absorption devices, *Finite Elements in Analysis and Design*, 91(1), 2014, 30-39.
- [15]. Tarigopula, V., Langseth, M., Hopperstad, O. S. and Clausen, A. H.: Axial crushing of thin-walled high-strength steel sections, *International Journal of Impact Engineering*, 32(1), 2006, 847-882.
- [16]. Kathiresan, M. and Manisekar, K.: Axial crush behaviours and energy absorption characteristics of aluminium and E-glass/epoxy over-wrapped aluminium conical frusta under low velocity impact loading, *Compos Structures*, 136(1), 2016, 86–100.
- [17]. Adam, H. and Stahl, T.: The whole is more than the sum of its parts, *Auto Technology*, 2(1), 2002, 69–71.
- [18]. Portillo-Oscar. and Romero-Luis-Eduardo.: Impact Performance of Advanced High Strength Steel Thin-Walled Columns, *Proceedings of the World Congress on Engineering*, Vol 2, 2008.
- [19]. Hu, L. L., He, X. L., Wu, G. P. and Yu, T. X.: Dynamic crushing of the circular-celled honeycombs under out-of-plane impact, *International Journal of Impact Engineering*, 75(1), 2015, 150–161.
- [20]. Xiong-Zhang., Hui-Zhang. and Zhuzhu-Wen.: Experimental and numerical studies on the crush resistance of aluminum honeycombs with various cell configurations, *International Journal of Impact Engineering*, 66(1), 2014, 48–59.
- [21]. Zhonggang-WANG., Shuguang-YAO. Zhaijun-L.U., David-Huic. and Luciano-Feo.: Matching Effect of Honeycomb-filled Thin-Walled Square Tube —Experiment and Simulation, *Composite Structures*, 57(1), 2016, 494–505.

-
- [22]. Qiang-Liu., Zhengwei-Mo., Yinghan-Wu., Jingbo-Ma., Gary-Chi-Pong-Tsui. and David-Hui.: Crush response of CFRP square tube filled with aluminum honeycomb, *Composites Part B*, 98(1), 2016, 406–414.
- [23]. Nasir Hussain, N., Srinivasa-Prakash-Regalla. and Venkata-Daseswara-Rao-Yendluri.: Numerical investigation into the effect of various trigger configurations on crashworthiness of GFRP crash boxes made of different types of cross sections, *International Journal of Crashworthiness*, 22(5), 2017, 565–581.